Published in final edited form as:
Pflugers Arch. 2009 March ; 457(5): 1023–1033. doi:10.1007/s00424-008-0570-x.

Sodium current properties of primary skeletal myocytes and cardiomyocytes derived from different mouse strains

M. Mille, **X. Koenig**, and **E. Zebedin**
Institute of Pharmacology, Center for Biomolecular Medicine and Pharmacology, Medical University of Vienna, Waehringerstrasse 13A, 1090 Vienna, Austria

P. Uhrin
Department of Vascular Biology and Thrombosis Research, Center for Biomolecular Medicine and Pharmacology, Medical University of Vienna, Waehringerstrasse 13A, 1090 Vienna, Austria

R. Cervenka, **H. Todt**, and **K. Hilber**
Institute of Pharmacology, Center for Biomolecular Medicine and Pharmacology, Medical University of Vienna, Waehringerstrasse 13A, 1090 Vienna, Austria

Abstract

The mouse has become the preferred animal for genetic manipulations. Because of the diverse genetic backgrounds of various mouse strains, these can manifest strikingly different characteristics. Here, we studied the functional properties of currents through voltage-gated sodium channels in primary cultures of skeletal myocytes and cardiomyocytes derived from the three commonly used mouse strains BL6, 129/Sv, and FVB, by using the whole-cell patch-clamp technique. We found strain-specific sodium current function in skeletal myocytes, which could partly be explained by differences in sodium channel isoform expression. In addition, we found significant effects of cell source (neonatal or adult animal-derived) and variation of the differentiation time period. In contrast to skeletal myocytes, sodium current function in cardiomyocytes was similar in all strains. Our findings are relevant for the design and proper interpretation of electrophysiological studies, which use excitable cells in primary culture as a model system.

Keywords

Sodium currents; Sodium channel isoforms; Skeletal myocytes; Cardiomyocytes; Primary cultures; Mouse strains

Introduction

The mouse is a major model organism in biomedical research, and because of technical and economical reasons, it has become the preferred animal for genetic manipulations. The use of genetically engineered mice has brought about considerable progress in various scientific fields; in the future, it will become more and more important for the study of physiological mechanisms, molecular mechanisms of disease, and for the evaluation of innovative therapeutic strategies.

karlheinz.hilber@meduniwien.ac.at.
M. Mille and X. Koenig contributed equally to this work.

Europe PMC Funders Author Manuscripts

The biomedical research community now has access to several hundreds of inbred mouse strains. Because of their diverse genetic backgrounds, these can manifest strikingly different characteristics. In consequence, experimental results may considerably vary, depending on the particular mouse strain chosen for a scientific study. Moreover, mutations and transgenes are often maintained on mixed genetic backgrounds of unspecific origin. Contempt of strain (or substrain) differences, e.g., between wild-type and knock-out mice to be compared, can lead to poor experimental design and faulty data interpretation. Finally, a specific genetic manipulation combined with genes unique to the background of a strain may generate a strain-specific phenotype, which is different from that in other strains. Consequently, for an adequate design of scientific studies using mice, for the proper choice of a suitable strain, and to correctly and unambiguously interpret genetic manipulations, it is mandatory to characterize potential strain-dependent properties.

Here, we studied the functional properties of currents through voltage-gated sodium channels in primary cultures of skeletal myocytes and cardiomyocytes derived from mice of the three very commonly used mouse strains C57BL/6 (BL6), 129/SvEvTacfBR (129), and FVB/NCr (FVB). Besides other applications, skeletal myocyte primary cultures are employed as a model system to compare the electrophysiological properties of muscles from wild-type and genetically manipulated mice (e.g., [1-3]). In addition, undifferentiated skeletal myocytes (myoblasts), derived from adult human skeletal muscle, are used in cell therapy approaches [4]. Primary mouse cardiomyocytes are considered a suitable model to investigate possible cardiac phenotypes of genetically manipulated mice [5]. We chose to study the functional properties of sodium currents for several reasons. First, whereas functional parameters of muscle contractility have already been compared between various mouse strains [6, 7], comparable studies on electrophysiological parameters in skeletal and cardiac muscle are lacking. Sodium channels rather than other ion channels were selected because their isoform and subunit expression profile in muscular tissues are far less complicated compared to that of other channels (e.g., calcium channels or potassium channels). This facilitated data interpretation. Secondly, abnormal sodium channel expression and/or function was reported in animal models of human skeletal muscle (e.g., [8-10]) and cardiac [11-13] diseases. Finally, a recent paper [14] provided evidence that sodium channel isoform expression is strain dependent in mouse cardiac ventricles. This may result in strain-specific sodium current function.

Materials and methods

Skeletal muscle and cardiac primary muscle cell preparation

Primary muscle cell cultures were prepared from healthy mice of different strains (C57BL/6, animal breeding facility in Himberg, Austria; 129/SvEvTacfBR, Taconic Farms, Germantown, NY, USA; FVB/NCr, NIH/NCI/DCT production facility, Frederick, MD, USA) in accordance with the protocol described in [15] and coinciding with the rules of the University Animal Welfare Committee. Skeletal myoblasts were isolated from the hind limbs of neonatal (1- to 4-day old) mice or the lower legs of female adult (12–24 weeks) mice. Cardiomyocytes were isolated from the hearts of neonatal (1–4 days) mice. Removed muscle tissues (skeletal muscle and/or cardiac muscle) were placed in a culture dish containing ice-cold growth medium (GM) consisting of Dulbecco's modified Eagle's medium (Invitrogen GmbH, Lofer, Germany) containing 4.5 g/l glucose, 4mM L-glutamine, 50 U/ml penicillin, 50 μg/ml streptomycin, and 20% fetal calf serum (PAA Labs. GmbH, Pasching, Austria). Thereafter, the muscle tissue was freed from connective tissue under microscopic control. The remaining muscle was mechanically dissociated in GM and repeatedly forced through the tip of a 10-ml pipette. Thereafter, the tissue homogenate was mixed 1:1 with a “solid tissue digestor” [RPMI-1640 medium, 10% fetal calf serum, 50 U/ml penicillin, 50 μg/ml streptomycin, 5 mM L-glutamin, 195 U/ml collagenase type I

(Sigma, Vienna, Austria)] in order to isolate satellite cells by proteolytic digestion. This mixture was shaken for 3 h at 37°C. Afterward, the cell suspension was centrifuged (1,200 rpm, 5 min), and the pellet was re-suspended in PBS. After another centrifugation step, the pellet was re-suspended in GM and, consecutively, filtered through a cell strainer (40 μm). The filtrate was centrifuged, and the pellet was again re-suspended in GM. Finally, this cell suspension was plated on Matrigel-coated (Becton Dickinson GmbH, Schwechat, Austria) culture dishes (3.5 cm, Sarstedt, Wiener Neudorf, Austria).

Cell culture

Primary skeletal myoblasts were incubated in GM at 37°C and 5% CO_2. As soon as about 70–80% of the culture dish surface was covered with proliferating myoblasts, cell differentiation was induced by incubation in differentiation medium (DM). This was identical to the GM, except that it contained 2% horse serum (Invitrogen) instead of 20% fetal calf serum. Incubation in DM (with reduced serum content) induced myoblast fusion and resulted in the generation of multi-nucleated myocytes. These myocytes exhibited either a spherical (myoballs) or a longitudinal shape (myotubes). The use of Matrigel-coated dishes guaranteed long-term survival of differentiated, spontaneously contracting myocytes (both myoballs and myotubes) as previously shown [16]; these cultures could be kept for at least 3 weeks without any obvious signs of deterioration. Media were changed three times per week. Primary cardiomyocytes were grown on Matrigel-coated dishes in GM for up to 1 week. The GM was changed three times per week.

Electrophysiology

Sodium currents were recorded from differentiated skeletal myocytes and cardiomyocytes at room temperature (22± 1.5°C) using an Axoclamp 200B patch-clamp amplifier (Axon Instruments, Union City, CA, USA) as in [16]. In case of the skeletal myocytes, the use of spherically shaped myoballs, rather than longitudinally shaped myotubes, guaranteed a proper voltage control in the whole-cell mode of the patch-clamp technique. Myoballs have previously been shown to resemble the electrophysiological properties of differentiated myotubes (e.g., [17]). Skeletal myocytes obtained from neonatal mice were used for measurements 3–6 days (early differentiation window) and 10–14 days (late differentiation window) after incubation in DM. The longer differentiation period was chosen to allow the cells to develop “mature” electrophysiological conditions, which has previously been shown to take longer than a week in skeletal myocytes [18-20]. Sodium currents of skeletal myocytes from adult mice were only recorded in the late differentiation window. Cardiomyocytes isolated from neonatal mouse hearts were used for measurements 1–4 days after preparation. These cells tended to spread out and become flatter with time in culture, which made measurements at later time periods impossible. A similar phenomenon is described in [5]. Pipettes were formed from aluminosilicate glass (AF150-100-10; Science Products, Hofheim, Germany) with a P-97 horizontal puller (Sutter Instruments, Novato, CA, USA), heat-polished on a micro-forge (MF-830; Narishige, Japan), and had resistances between 1 and 2 MΩ when filled with the recording pipette solution (105 mM CsF, 10 mM NaCl, 10 mM EGTA, 10 mM HEPES, pH=7.3). Voltage-clamp protocols and data acquisition were performed with pclamp 6.0 software (Axon Instruments) through a 12-bit A–D/D–A interface (Digidata 1200; Axon Instruments). Data were low-pass-filtered at 2 kHz (−3 dB) and digitized at 10–20 kHz. Curve fitting was performed using ORIGIN 7.0 software (MicroCal Software, Northampton, MA, USA). Sodium current recording was always begun about 5 min after whole-cell access was attained in order to minimize time-dependent shifts in channel gating. In addition, in order to avoid such shifts to systematically influence our experiments (e.g., comparisons between different mouse strains), the following temporal experimental sequence was always strictly retained for each cell: detection of the current–voltage relationship, followed by recording of the capacitive current

transient, steady-state fast inactivation, steady-state slow inactivation, and finally, superfusion with 1 μM tetrodotoxin (TTX). Current–voltage (*IV*) relationships were fit with function F1: $I/I_{max}=G_{max}\times(V-V_{rev})/(1+\exp((V_{0.5}-V)/K))$, where I/I_{max} is the normalized current, G_{max} is the maximum conductance divided by I_{max}, V is the membrane potential, V_{rev} is the reversal potential, $V_{0.5}$ is the voltage at which half-maximum activation occurred, and K is the slope factor. Decay half-time, a measure of fast inactivation kinetics, was obtained by analyzing the time period between the current peak and the time point at which the current had decayed to 50%. Sodium current density was calculated by dividing the maximum peak inward current amplitude of a cell by its membrane capacitance [16]. Cell capacitance was measured by integrating the area under the capacitive transient elicited by a 10-ms voltage step from −120 to −80 mV, which did not activate any channels. This value was then divided by the applied voltage change (40 mV). Steady-state fast inactivation data were fit with the Boltzmann function F2: $I/I_{max}=1/(1+\exp((V-V_{0.5})/K))$, where I/I_{max} is the normalized current, V is the membrane potential, $V_{0.5}$ is the voltage at which half-maximum inactivation occurred, and K is the slope factor. Steady-state slow inactivation data were fit with function F3: $I/I_{max}=1-Fract_{SI}/(1+\exp((V_{0.5}-V)/K))$, where $Fract_{SI}$ is the final current level reached at depolarized potentials, representing the fraction of channels, which are slow inactivated. Recordings were made in a bath solution that consisted of 140 mM NaCl, 2.5 mM KCl, 1 mM $CaCl_2$, 1 mM $MgCl_2$, 10 mM HEPES, pH=7.4. Some experiments were executed in low sodium bath solution containing 15 mM Na^+ in order to minimize current amplitudes. In this case, 125 mM Na^+ was substituted by the impermeant monovalent cation *N*-methyl-D-glucamine. Chemicals were purchased from Sigma. TTX (1 μM) in the bath solution was used to eliminate TTX-sensitive sodium currents and allowed an estimation of the TTX-resistant sodium channel fractions present in the cells. Rapid solution changes were performed by a DAD-8-VC superfusion system (ALA Scientific Instruments, Westbury, NY, USA).

Data are expressed as means±SE. Statistical comparisons were made using ANOVA (for independent samples) when more than two groups had to be compared and two-tailed Student's unpaired *t* tests for comparison of two groups. A $p<0.05$ was considered significant and a $p<0.01$, highly significant.

Results

Sodium current properties of primary skeletal myocytes derived from different mouse strains

Current–voltage (*IV*) relationships of the sodium currents in skeletal myocytes derived from BL6, 129, and FVB mice were obtained by application of depolarizing voltage steps between −90 and +55 mV from a holding potential of −120 mV. Thereafter, the peaks of the elicited sodium currents were plotted against the applied potentials. The myocytes were derived from neonatal or adult mice and cultured in DM for 3–6 days (early differentiation window) or 10–14 days (late differentiation window). In neonatal animal-derived cells of both differentiation windows, the *IV* relationships of BL6 and 129 were very similar. In contrast, the *IV* relationship of FVB-derived cells was shifted to the right. To obtain quantitative parameters for comparison (Table 1), the *IV* relationships were fit with function F1 given in the “Materials and methods”. This revealed a significant shift of $V_{0.5,}$ the voltage at which half-maximum activation occurs toward more positive potentials in FVB-derived compared to BL6- and 129-derived cells. In addition, K, the slope factor of the *IV* relationship, was significantly increased in FVB-derived cells. This reflects a reduced voltage dependence of activation compared to BL6-and 129-derived cells. Finally, the reversal potentials (V_{rev} values) of cells derived from neonatal mice were similar in all strains, except for a moderate reduction of this value in FVB-derived cells of the late differentiation window (Table 1). In contrast to the described strain differences in the *IV*

relationship parameters of cells derived from neonatal mice, no significant differences between the strains could be found in cells derived from adult animals (Table 1).

Brief depolarizations (≤50 ms) also cause, besides activation, inactivation of sodium channels from which they recover with a single kinetic phase, whose time constant is on the order of a few milliseconds. This inactivation process is called sodium channel “fast inactivation”. The kinetics of the development of fast inactivation is represented by the speed of the current decay following channel activation. In Fig. 1 (top left image), original traces of current decay are displayed on an expanded time scale. The current decays following activation by a voltage step, which elicited the maximum current (current decay at I_{max}), were compared between cells derived from neonatal mice of different strains in the late differentiation window. It can be noticed that current decay was faster in FVB (empty triangles) than in the other strains. Quantitative kinetic values were obtained by analyzing the time period between the current peak and the time point at which the current had decayed to 50% (decay half-time, see arrows in Fig. 1). First, current decays at I_{max} were analyzed. We found that the decay half-times in neonatal animal-derived FVB cells were significantly decreased compared to those in the other strains in both differentiation windows (Table 1). In contrast to neonatal animal-derived cells, no significant strain differences could be found in the current decays of adult animal-derived cells (Table 1). Here, 129-derived cells only showed a tendency toward slowed current decay. Because open state inactivation is known to be a function of voltage, in addition to current decay half-times at I_{max}, the current decays at various potentials were also analyzed (Fig. 1). It can be noticed that in neonatal animal-derived cells of the early differentiation window (neonatal early), current decay was similar in all strains over the whole voltage range displayed. Thus, the significantly speeded current decay at I_{max} of FVB cells in this differentiation window (Table 1) was simply due to the fact that the IV relationship in this strain was shifted toward more positive voltages (Table 1). In contrast, in neonatal animal-derived cells of the late differentiation window (neonatal late), significant differences in current decay existed between the strains at depolarized voltages, whereby FVB cells showed the fastest decay (Fig. 1). Finally, in adult animal-derived cells, current decay was found significantly slower at various but not all voltages in 129 compared to the other strains (Fig. 1).

Kinetic parameters of sodium channel activation or fast inactivation (e.g., current decay), detected using the whole-cell patch-clamp technique, may be influenced by technical problems such as an insufficient control over the membrane voltage [21]. This is especially true for measurements on big and nonspherical cells. Consequently, systematic differences in cell size, e.g., between the cell populations derived from different strains, may have affected our current decay measurements. To check for this, we compared membrane capacitance, a measure of cell size, in myocytes derived from BL6, 129, and FVB mice. In general, the capacitance values were similar. A single significant strain difference was found for neonatal animal-derived FVB cells in the early differentiation window when compared to the other two strains (Table 1). To make sure that cell size differences did not affect our current decay data, membrane capacitance and decay half-times at I_{max} were correlated with each other. A linear regression model was used, which revealed no significant correlation between membrane capacitance and decay half-time in any strain. The respective values of the correlation coefficient, r^2, ranged from 0.0003 to 0.0754 (0.03±0.02; mean±SE) in BL6 cells, 0.0069–0.0532 (0.02±0.02) in 129 cells, and 0.0122–0.2061 (0.08±0.06) in FVB cells. Based upon these values, it can be concluded that cell size did not influence the current decay measurements in this study. In addition to the capacitance values, the current densities were estimated for myocytes derived from the three strains. Generally, they were similar, except for a significantly increased current density in neonatal animal-derived BL6 cells of the late differentiation window compared to FVB cells (Table 1).

The left part of Table 2 shows a comparison of the voltage dependencies of sodium current fast inactivation in skeletal myocytes derived from neonatal and adult BL6, 129, and FVB mice. To obtain steady-state fast inactivation curves, from a holding potential of −120 mV, 50-ms inactivating prepulses to various potentials (−110 to −30 mV) were applied. The peaks of the currents elicited by immediately following test pulses to −20 mV were then plotted against the prepulse voltage. We found that fast inactivation parameters were generally similar in all strains. However, statistical analysis revealed several significant differences of minor dimension in $V_{0.5}$, the voltage at which half-maximum fast inactivation occurred, and K, the slope factor of the steady-state inactivation curve. These existed between FVB- and BL6-derived cells and between FVB-and 129-derived cells (see Table 2). Taken together, the voltage dependencies of fast inactivation were similar in all strains both in neonatal and adult animal-derived cells.

Prolonged depolarizations (seconds to minutes) cause inactivation of sodium channels from which they recover with multiple kinetic phases, whose time constants range over several orders of magnitude from tens of milliseconds up to tens of seconds. These kinetic phases of recovery can be summarized by the term “slow inactivation”. To test for the voltage dependence of slow inactivation, from a holding potential of −120 mV, 10-s prepulses to various potentials (−110–0 mV) were applied to slow inactivate the channels. Thereafter, a 20-ms repolarization to −140 mV was applied in order to allow the channels to recover from fast inactivation. The peaks of the currents elicited by immediately following test pulses to −20 mV were then plotted against the prepulse voltage to obtain steady-state slow inactivation curves. We found striking differences between the voltage dependencies of sodium current slow inactivation in skeletal myocytes derived from neonatal BL6, 129, and FVB mice. First, in the early differentiation window, the steady-state inactivation curve of 129-derived cells was strongly shifted to more negative potentials compared to that of cells derived from the two other strains. This is represented by a 10-mV left-shift in the voltage at which half-maximum slow inactivation occurred ($V_{0.5}$ value, Table 2) in 129-derived cells. Secondly, in the late differentiation window, the fraction of channels, which can be slow inactivated (Fract_{SI}), showed a pronounced strain dependence, with the largest Fract_{SI} values found in FVB-derived cells and the lowest values found in BL6-derived cells (Table 2). This indicates that the sodium currents of BL6-derived cells were most resistant to the process of slow inactivation. FVB-derived cells, on the other hand, were most susceptible to slow inactivation. In contrast to neonatal animal-derived cells, no significant strain differences could be found in the voltage dependencies of slow inactivation in adult animal-derived cells (Table 2).

Besides the main comparison between the sodium current parameters of skeletal myocytes derived from different mouse strains described above, Tables 1 and 2 also provide a comparison between neonatal and adult animal-derived cells (compare lines “neonatal late” with “adult”), as well as a comparison between myocytes, which were incubated in DM for a short (early differentiation window) and a longer (late differentiation window) time period (compare lines “neonatal early” with “neonatal late”).

Various sodium current parameters were significantly different between neonatal and adult animal-derived cells. These differences were strain dependent and are listed below, including the p values of Student's t tests, which are missing in Tables 1 and 2. In cells derived from BL6 and FVB mice, the IV relationship of adult preparations was significantly shifted ($V_{0.5}$ values, $p<0.01$) toward more negative potentials (Table 1). In addition, only in FVB-derived cells, besides $V_{0.5}$, were the K and V_{rev} values also significantly different between neonatal and adult preparations ($p<0.01$). Current decay at I_{max} generally tended to be slower in cells derived from adult animals in all strains. Here, statistical significance was reached in FVB ($p<0.01$) and 129 ($p<0.05$; Table 1). A difference ($p<0.05$) also existed in

the current densities in BL6-derived cells, with a higher current density in neonatal preparations (Table 1). This difference, however, seems to be a result of a longer differentiation time of neonatal cells (compare lines neonatal early with neonatal late; see next paragraph) rather than a specific feature of neonatal versus adult cells. In accordance, [22] demonstrated that sodium channel mRNA levels increase during cultivation of embryonic rat skeletal myocytes. For steady-state fast inactivation parameters, in BL6- and 129-derived cells, $V_{0.5}$ was significantly shifted toward more negative potentials in adult preparations, with p values <0.05 and <0.01, respectively (Table 2). Finally, the only significant difference (p<0.05) in the steady-state slow inactivation curves of neonatal and adult animal-derived cells existed in the $Fract_{SI}$ values of the BL6 strain, where adult preparations showed a higher value (Table 2).

Comparison between the sodium current parameters of neonatal animal-derived skeletal myocytes in the *early* and the *late differentiation window* also revealed some significant differences, which were in part strain dependent. Here, the *IV* relationships displayed differences in all strains. Namely, the $V_{0.5}$ values were consistently shifted toward more negative potentials (p<0.05 in BL6 and p<0.01 in 129 and FVB; Table 1) in the late differentiation window. In addition, the steepness of the *IV* relationships was increased (smaller K values) in the late window, reaching statistical significance only in 129 (p<0.01) and FVB (p<0.05). Finally, the V_{rev} values were significantly less positive (p<0.01) in the late window in the FVB strain (Table 1). In all strains, current decay at I_{max} tended to be slower in cells from the late differentiation window, whereby statistical significance (p<0.01) was only reached in the 129 strain (Table 1). Current densities in the late window were significantly higher (p<0.05) only in the BL6 strain (Table 1). The steady-state fast inactivation curves were significantly shifted (p<0.01) toward more negative potentials in the late window only in FVB (Table 2). Moreover, their K values were significantly increased (p<0.05) in the late window in 129 (Table 2). Finally, comparison of the steady-state slow inactivation curves in the early and late differentiation window revealed that $V_{0.5}$ was significantly shifted (p<0.01) toward more positive potentials in the late window only in 129 (Table 2). The $Fract_{SI}$ values were decreased in the late window in all strains (Table 2). Here, statistical significance was reached in BL6 (p<0.01) and 129 (p<0.05).

Taken together, both cell source (neonatal or adult animal-derived) and differentiation time period can significantly affect the sodium current properties of skeletal myocytes in primary culture.

Sodium channel isoform expression as possible source for strain-specific sodium current properties

Besides the adult skeletal muscle sodium channel isoform $Na_v1.4$, primary skeletal myocyte cultures also express $Na_v1.5$ channels (e.g., [23, 24]), which are otherwise expressed only in developing or denervated skeletal muscle and in the heart. Because these two sodium channel isoforms significantly differ in their functional properties (e.g., [25-28]), distinctions in their expression levels may account for the mouse strain-specific sodium channel properties observed in this study.

To test for differences in sodium channel isoform expression, we compared the TTX sensitivities of sodium currents in skeletal myocytes derived from the different mouse strains. It is well known that the currents through $Na_v1.5$ channels are more resistant to TTX block than those through $Na_v1.4$ channels; thus, a shift in sodium channel isoform expression from $Na_v1.4$ toward $Na_v1.5$ should result in a reduced TTX sensitivity. Figure 2 shows a typical TTX experiment carried out on a neonatal animal-derived BL6 cell in the early differentiation window: Sodium currents were first measured under control conditions. Thereafter, 1 μM TTX was washed in, and the currents were detected again. A final current

measurement was performed after TTX was washed out. It can be noticed that 1 μM TTX significantly reduced the current amplitudes, leaving a current carried by a "TTX-resistant" sodium channel fraction. This fraction most probably represents current through $Na_v1.5$ channels (IC_{50}~1μM) because $Na_v1.4$ channels (IC_{50}~10 nM) should be totally blocked by 1μM TTX (e.g., [24, 29]). Table 3 displays the TTX-resistant sodium current fractions for cells derived from the different mouse strains. In neonatal animal-derived cells, this fraction was significantly increased in 129 compared to the two other strains. This suggests a greater contribution of $Na_v1.5$ to the total sodium current in 129-derived cells. In contrast to neonatal animal-derived cells, the TTX-resistant current fractions were similar in all strains in adult preparations (Table 3).

Sodium current properties of primary cardiomyocytes derived from different mouse strains

The upper image of Fig. 3a shows typical sodium currents and the corresponding *IV* relationship of a cardiomyocyte derived from the heart of a neonatal 129 mouse. Compared to neonatal animal-derived skeletal myocyte currents (top of Fig. 3b), the cardiomyocyte currents exhibited slower kinetics (see also Table 1). Another well-defined sodium current speciality of cardiomyocytes is their high resistance to slow inactivation. The lower image of Fig. 3a shows that about 60% of the total current remained after 10-s prepulses to strongly depolarized potentials. This suggests that 60% of the channels in this cardiomyocyte could not be slow inactivated (see also Table 1). In the skeletal myocyte (bottom of Fig. 3b), only about 30% of the channels were resistant to slow inactivation.

In order to compare the sodium current properties in cardiomyocytes derived from the different mouse strains, the same experiments were performed on cardiomyocytes as described above for skeletal myocytes. The respective sodium current parameters obtained on cardiomyocytes derived from the three strains are given in the Tables 1 and 2. It can be noticed that, in contrast to those of neonatal animal-derived skeletal myocytes, the sodium current properties of cardiomyocytes were hardly strain dependent. This was true for the activation parameters, the inactivation kinetics, and the current densities (Table 1), as well as for the voltage dependencies of fast and slow inactivation (Table 2). A few significant differences of minor dimension, however, could be detected. Namely, the *K* value of the *IV* relationship was decreased in FVB- compared to BL6-derived cells (Table 1), and the *K* value of the steady-state slow inactivation curve was slightly increased in 129 compared to the two other strains (Table 2).

Discussion

In the present study, we compared the functional properties of sodium currents in primary skeletal myocytes and cardiomyocytes derived from three commonly used mouse strains. To avoid confusion, it should be clearly pointed out that we did not investigate strain-specific differences in the function and expression of sodium channels in neonatal and adult skeletal muscle or in the neonatal heart. In fact, strain-specific responses of primary skeletal myocytes and cardiomyocytes to cultivation were studied. Such primary cultures serve as model system to study the properties of muscle tissues (e.g., [1-3, 5]).

Mouse strain effects

Previous reports have shown that ion channel expression in various tissues can considerably differ between mice of different strains. For example, a dramatic difference was found in cerebellar $K_v1.2$ potassium channel expression and cellular localization between BL6 and 129 mice [30]. Similarly, [14] reported strain-specific sodium and potassium channel isoform expression in mouse cardiac ventricles, and [31] found strain-specific TRP channel

expression in various tissues, including skeletal muscle. Our investigation adds functional data to these studies, which exclusively focused on ion channel expression. We found strain-specific sodium channel function in primary skeletal myocytes derived from neonatal mice. Thus, besides strain-dependent ion channel expression [14, 30, 31], the functional properties of ion channels (this study), which determine cellular excitability, can also differ between cells of various strains. Similar to our electrophysiological study, other authors also found functional properties of muscular tissues to be clearly mouse strain dependent. For example, the response to exercise training was dramatically increased in FVB mice compared with that in other strains [6]. Moreover, whereas cardiac contractile function was similar under physiological conditions, significant strain differences were exposed at sub-physiological temperature and frequency [7]. Together, these studies [6, 7] and our data support the concept that important functional properties of muscular tissues can be significantly different in various mouse strains.

What is the cause for strain-dependent sodium current function in neonatal animal-derived skeletal myocytes? The fact that primary skeletal myocytes express both $Na_v1.4$ and $Na_v1.5$ channels (e.g., [23, 24]), which are functionally different (e.g., [25-28]), prompted us to test the hypothesis that shifts in the expression of these sodium channel isoforms generate strain-specific sodium current function. Indeed, we found differences in the TTX sensitivities between neonatal animal-derived cells of various strains, suggesting strain-specific sodium channel isoform expression. However, these differences did not always closely correlate with the sodium current parameters detected. Namely, with regard to the sodium current parameters, the FVB strain was outstanding and differed from 129 and BL6. For example, in FVB cells, activation was shifted to more positive potentials, and, at least in the late differentiation window, current decay was speeded, and the fraction of channels that could be slow inactivated was increased. Considering the specific functional properties of $Na_v1.4$ and $Na_v1.5$ when expressed in a given cell type (e.g., [25-28]), all these shifts in sodium current parameters could be explained by a higher contribution of $Na_v1.4$ to the total sodium current in FVB cells compared to 129 and BL6 cells. In the corresponding TTX data, however, the 129 strain was outstanding in that it showed a greater TTX-resistant current fraction compared to FVB and BL6, concomitant with a higher contribution of $Na_v1.4$ in both FVB and BL6 cells. This partial inconsistency between the sodium current and the TTX data prompts us to conclude that strain-specific expression of $Na_v1.4$ and $Na_v1.5$ channels may be one but not the only cause for strain-specific sodium current function in neonatal animal-derived skeletal myocytes. Among other possible reasons are differences in sodium channel β-subunit expression or different cellular protein kinase activities, which would result in altered sodium channel phosphorylation levels.

Finally, it is important to note that we found considerable strain differences only in neonatal animal-derived but not in adult animal-derived skeletal myocytes. Interestingly, the TTX sensitivities were also similar between the strains in adult animal-derived cells. This finding argues for an involvement of sodium channel isoform expression shifts in the generation of strain-specific sodium current functional properties. The reason for this basic difference between neonatal and adult animal-derived cells is currently unknown.

In contrast to skeletal myocytes, we did not find major strain differences in the sodium current properties of primary cardiomyocytes derived from neonatal mice. This seems to contradict [14], who, using the same mouse strains as in the present study, reported significant effects of the genetic background on sodium channel transcripts in mouse cardiac ventricles. Namely, the FVB strain expressed less $Na_v1.5$ transcripts but more $Na_v1.4$, $Na_v1.3$, and $Na_vβ$ transcripts than 129 and BL6. One might expect that such expression shifts of sodium channel isoforms (with different functional properties) in cardiomyocytes should alter their sodium current parameters. However, although significant, the strain

differences in sodium channel isoform expression described in [14] were rather small, with $Na_v1.5$ still representing by far the dominating isoform in all strains. This is consistent with our finding of similar sodium channel function in cardiomyocytes derived from FVB, 129, and BL6 mice. Furthermore, a direct comparison between the results of [14] and our study is not valid because adult mouse cardiac ventricles and primary cardiomyocyte cultures, respectively, were used. Besides the study of [14], there is also evidence that cardiac electrophysiological properties are different in various mouse strains. Thus, [32] and [33] reported strain-dependent ECG characteristics, and [34] found differences in the vulnerability to ventricular arrhythmia between various strains. Strain-specific ion channel expression and/or function of cardiomyocytes [14] in various regions of the heart are likely to cause such electrophysiological differences. Our data suggest that sodium channels might not considerably contribute. Of course, this is only true if the electrophysiological properties of cardiomyocytes in primary culture are similar to those of adult cardiomyocytes. Although not directly compared in [5], such a conclusion was drawn by these authors.

Relevance of the study

Several of our findings are relevant for the design and proper interpretation of electrophysiological studies, which use excitable cells in primary culture as a model system: First, cells derived from different mouse strains can exhibit different ion channel function and expression. Secondly, differences exist between neonatal and adult animal-derived cells, and finally, prolonged differentiation time periods do also affect the functional properties of the channels. Thus, experimental design, comparisons of the results between studies, and data interpretation should be done very carefully. For example, contempt of strain differences, e.g., between wild-type and knock-out mice to be compared, may lead to faulty data interpretation. Namely, strain differences in a certain electrophysiological parameter, but not differences due to the genetic manipulation itself, may be artificially exposed.

In accordance with previous studies (e.g., [22-24]), our data imply that primary skeletal myocyte cultures do not represent an appropriate model system to explore the electrophysiological properties of adult skeletal muscle. Independent of the mouse strain used for cell isolation and independent of the differentiation time period in culture, both myocytes derived from neonatal and adult skeletal muscle express a large fraction of $Na_v1.5$ channels, which are normally absent in adult skeletal muscle [22, 35]. This is suggested by the fact that application of 1 μM TTX reduced the sodium current to 30–40%, which implies that 60–80% of the active channels in the cultures were TTX-resistant $Na_v1.5$ channels (assuming an IC_{50} value of 1 μM for $Na_v1.5$).

In contrast to primary skeletal myocyte cultures, which obviously fail as a model for adult skeletal muscle, the electrophysiological properties of primary cardiomyocyte cultures derived from neonatal mice may be similar to those of adult cardiac tissue [5]. In addition, neonatal mouse cardiomyocytes in primary culture have a small cell size and lack transverse tubules, which makes them technically favorable for whole-cell patch-clamp studies when compared to freshly isolated adult cardiomyocytes [5]. Taken together with our finding that sodium current function in neonatal primary cardiomyocytes is not strain dependent, this preparation promises to be a suitable model to investigate possible cardiac phenotypes of genetically manipulated mice.

Acknowledgments

Financial support was provided by a grant from the Austrian Science Fund (FWF, P19352-B11). We are grateful to Martina Molin for the excellent technical assistance.

References

1. Burton KA, Johnson BD, Hausken ZE, Westenbroek RE, Idzerda RL, Scheuer T, Scott JD, Catterall WA, McKnight GS. Type II regulatory subunits are not required for the anchoring-dependent modulation of Ca2+ channel activity by cAMP-dependent protein kinase. Proc Natl Acad Sci U S A. 1997; 94:11067–11072. [PubMed: 9380760]
2. Ahern CA, Sheridan DC, Cheng W, Mortenson L, Nataraj P, Allen P, De WM, Coronado R. Ca2+ current and charge movements in skeletal myotubes promoted by the beta-subunit of the dihydropyridine receptor in the absence of ryanodine receptor type 1. Biophys J. 2003; 84:942–959. [PubMed: 12547776]
3. Johnson BD, Scheuer T, Catterall WA. Convergent regulation of skeletal muscle Ca2+ channels by dystrophin, the actin cytoskeleton, and cAMP-dependent protein kinase. Proc Natl Acad Sci U S A. 2005; 102:4191–4196. [PubMed: 15753322]
4. Menasche P. Skeletal myoblasts as a therapeutic agent. Prog Cardiovasc Dis. 2007; 50:7–17. [PubMed: 17631434]
5. Nuss HB, Marban E. Electrophysiological properties of neonatal mouse cardiac myocytes in primary culture. J Physiol. 1994; 479(2):265–279. [PubMed: 7799226]
6. Massett MP, Berk BC. Strain-dependent differences in responses to exercise training in inbred and hybrid mice. Am J Physiol Regul Integr Comp Physiol. 2005; 288:R1006–R1013. [PubMed: 15618348]
7. Stull LB, Hiranandani N, Kelley MA, Leppo MK, Marban E, Janssen PM. Murine strain differences in contractile function are temperature- and frequency-dependent. Pflugers Arch. 2006; 452:140–145. [PubMed: 16397793]
8. Ribaux P, Bleicher F, Couble ML, Amsellem J, Cohen SA, Berthier C, Blaineau S. Voltage-gated sodium channel (SkM1) content in dystrophin-deficient muscle. Pflugers Arch. 2001; 441:746–755. [PubMed: 11316257]
9. Reddy S, Mistry DJ, Wang QC, Geddis LM, Kutchai HC, Moorman JR, Mounsey JP. Effects of age and gene dose on skeletal muscle sodium channel gating in mice deficient in myotonic dystrophy protein kinase. Muscle Nerve. 2002; 25:850–857. [PubMed: 12115974]
10. Filatov GN, Rich MM. Hyperpolarized shifts in the voltage dependence of fast inactivation of Nav1.4 and Nav1.5 in a rat model of critical illness myopathy. J Physiol. 2004; 559:813–820. [PubMed: 15254148]
11. Lee HC, Patel MK, Mistry DJ, Wang Q, Reddy S, Moorman JR, Mounsey JP. Abnormal Na channel gating in murine cardiac myocytes deficient in myotonic dystrophy protein kinase. Physiol Genomics. 2003; 12:147–157. [PubMed: 12454205]
12. Fredj S, Sampson KJ, Liu H, Kass RS. Molecular basis of ranolazine block of LQT-3 mutant sodium channels: evidence for site of action. Br J Pharmacol. 2006; 148:16–24. [PubMed: 16520744]
13. Hesse M, Kondo CS, Clark RB, Su L, Allen FL, Geary-Joo CT, Kunnathu S, Severson DL, Nygren A, Giles WR, Cross JC. Dilated cardiomyopathy is associated with reduced expression of the cardiac sodium channel Scn5a. Cardiovasc Res. 2007; 75:498–509. [PubMed: 17512504]
14. Demolombe S, Marionneau C, Le BS, Charpentier F, Escande D. Functional genomics of cardiac ion channel genes. Cardiovasc Res. 2005; 67:438–447. [PubMed: 15919067]
15. Zebedin E, Mille M, Speiser M, Zarrabi T, Sandtner W, Latzenhofer B, Todt H, Hilber K. C2C12 skeletal muscle cells adopt cardiac-like sodium current properties in a cardiac cell environment. Am J Physiol Heart Circ Physiol. 2007; 292:H439–H450. [PubMed: 16980339]
16. Zebedin E, Sandtner W, Galler S, Szendroedi J, Just H, Todt H, Hilber K. Fiber type conversion alters inactivation of voltage-dependent sodium currents in murine C2C12 skeletal muscle cells. Am J Physiol Cell Physiol. 2004; 287:C270–C280. [PubMed: 15044148]
17. Boldin S, Jager U, Ruppersberg JP, Pentz S, Rudel R. Cultivation, morphology, and electrophysiology of contractile rat myoballs. Pflugers Arch. 1987; 409:462–467. [PubMed: 3627962]

18. Sherman SJ, Lawrence JC, Messner DJ, Jacoby K, Catterall WA. Tetrodotoxin-sensitive sodium channels in rat muscle cells developing in vitro. J Biol Chem. 1983; 258:2488–2495. [PubMed: 6296148]
19. Caffrey JM, Brown AM, Schneider MD. Ca2+ and Na+ currents in developing skeletal myoblasts are expressed in a sequential program: reversible suppression by transforming growth factor beta-1, an inhibitor of the myogenic pathway. J Neurosci. 1989; 9:3443–3453. [PubMed: 2552033]
20. Liberona JL, Caviedes P, Tascon S, Hidalgo J, Giglio JR, Sampaio SV, Caviedes R, Jaimovich E. Expression of ion channels during differentiation of a human skeletal muscle cell line. J Muscle Res Cell Motil. 1997; 18:587–598. [PubMed: 9350011]
21. Bar-Yehuda D, Korngreen A. Space-clamp problems when voltage clamping neurons expressing voltage-gated conductances. J Neurophysiol. 2008; 99:1127–1136. [PubMed: 18184885]
22. Yang JS, Bennett PB, Makita N, George AL, Barchi RL. Expression of the sodium channel beta 1 subunit in rat skeletal muscle is selectively associated with the tetrodotoxin-sensitive alpha subunit isoform. Neuron. 1993; 11:915–922. [PubMed: 8240813]
23. Gonoi T, Sherman SJ, Catterall WA. Voltage clamp analysis of tetrodotoxin-sensitive and -insensitive sodium channels in rat muscle cells developing in vitro. J Neurosci. 1985; 5:2559–2564. [PubMed: 2411888]
24. Weiss RE, Horn R. Functional differences between two classes of sodium channels in developing rat skeletal muscle. Science. 1986; 233:361–364. [PubMed: 2425432]
25. Wang DW, George AL Jr. Bennett PB. Comparison of heterologously expressed human cardiac and skeletal muscle sodium channels. Biophys J. 1996; 70:238–245. [PubMed: 8770201]
26. O'Reilly JP, Wang SY, Kallen RG, Wang GK. Comparison of slow inactivation in human heart and rat skeletal muscle Na+ channel chimaeras. J Physiol. 1999; 515(1):61–73. [PubMed: 9925878]
27. Sheets MF, Hanck DA. Gating of skeletal and cardiac muscle sodium channels in mammalian cells. J Physiol. 1999; 514(2):425–436. [PubMed: 9852324]
28. Vilin YY, Makita N, George AL Jr. Ruben PC. Structural determinants of slow inactivation in human cardiac and skeletal muscle sodium channels. Biophys J. 1999; 77:1384–1393. [PubMed: 10465750]
29. Zimmer T, Bollensdorff C, Haufe V, Birch-Hirschfeld E, Benndorf K. Mouse heart Na+ channels: primary structure and function of two isoforms and alternatively spliced variants. Am J Physiol Heart Circ Physiol. 2002; 282:H1007–H1017. [PubMed: 11834499]
30. Connor JX, McCormack K, Pletsch A, Gaeta S, Ganetzky B, Chiu SY, Messing A. Genetic modifiers of the Kv beta2-null phenotype in mice. Genes Brain Behav. 2005; 4:77–88. [PubMed: 15720404]
31. Kunert-Keil C, Bisping F, Kruger J, Brinkmeier H. Tissue-specific expression of TRP channel genes in the mouse and its variation in three different mouse strains. BMC Genomics. 2006; 7:159. [PubMed: 16787531]
32. Appleton GO, Li Y, Taffet GE, Hartley CJ, Michael LH, Entman ML, Roberts R, Khoury DS. Determinants of cardiac electrophysiological properties in mice. J Interv Card Electrophysiol. 2004; 11:5–14. [PubMed: 15273447]
33. Brouillette J, Rivard K, Lizotte E, Fiset C. Sex and strain differences in adult mouse cardiac repolarization: importance of androgens. Cardiovasc Res. 2005; 65:148–157. [PubMed: 15621042]
34. Maguire CT, Wakimoto H, Patel VV, Hammer PE, Gauvreau K, Berul CI. Implications of ventricular arrhythmia vulnerability during murine electrophysiology studies. Physiol Genomics. 2003; 15:84–91. [PubMed: 12888626]
35. Trimmer JS, Cooperman SS, Agnew WS, Mandel G. Regulation of muscle sodium channel transcripts during development and in response to denervation. Dev Biol. 1990; 142:360–367. [PubMed: 2175278]

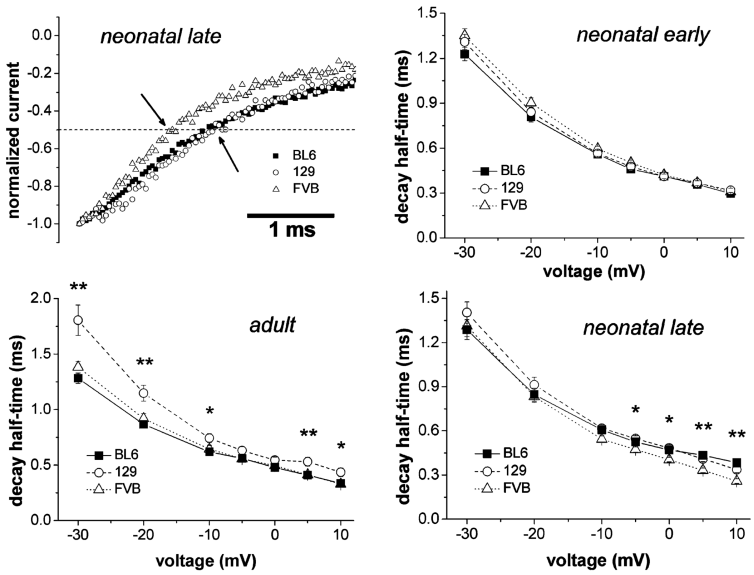

Fig. 1.

Comparison of the current decay kinetics in skeletal myocytes derived from different mouse strains. Typical examples of current decay at I_{max} are displayed in the *top left image*. The *arrows* indicate the time points at which current decay half-times were measured. These represent the time periods between the current peak and the time point at which the current had decayed to 50%. In the graphs, current decay half-times were plotted against the membrane voltage (steps between −30 and +10 mV from a holding potential of −120 mV) for myocytes derived from neonatal (early and late differentiation window) and adult mice. The lines connect single data points. Data are expressed as means±SE. *p<0.05 and **p<0.01 indicate a significant difference between the three strains at certain potentials revealed by ANOVA

Europe PMC Funders Author Manuscripts

Europe PMC Funders Author Manuscripts

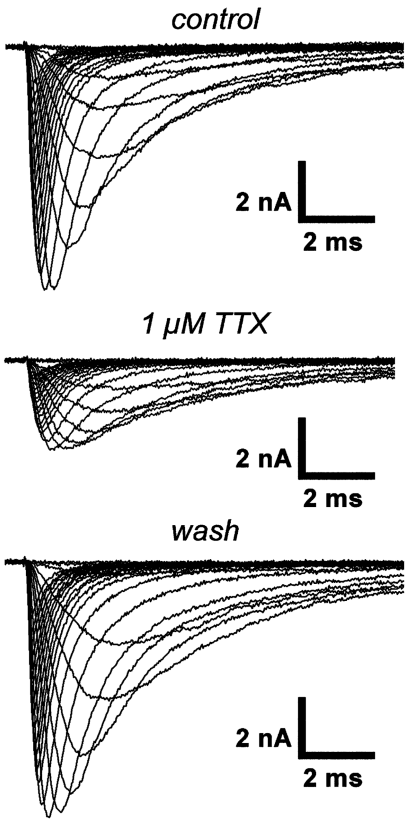

Fig. 2.

Sequential program and original traces of a typical TTX experiment. The currents were elicited by depolarizing voltage steps between −90 and +50 mV from a holding potential of −120 mV and were recorded from a skeletal myocyte in the early differentiation window derived from a neonatal BL6 mouse in 140 mM sodium bath solution. This ensured adequate current amplitudes also in the presence of 1 μM TTX. Currents during superfusion with bath solution containing 1 μM TTX were recorded 60 s after TTX application was begun

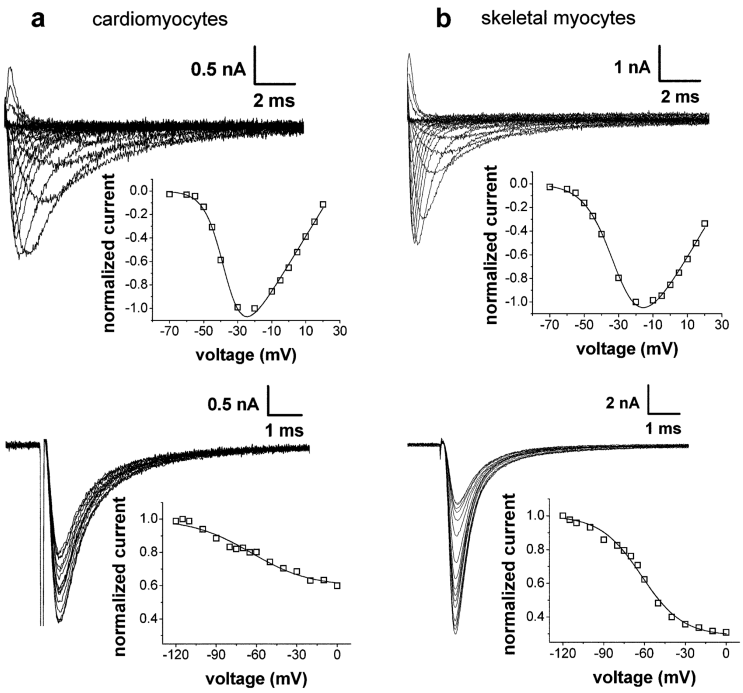

Fig. 3.

Typical examples of original current traces with the corresponding *IV* relationships (*upper panel*) and steady-state slow inactivation curves (*lower panel*) of cardiomyocytes (**a**) and skeletal myocytes (**b**) of the 129 strain. The experiments were performed on cardiomyocytes derived from neonatal mice and from skeletal myocytes derived from neonatal mice in the early differentiation window. The pulse protocols used to elicit the currents are given in the text of the "Results", and the fitting procedures (function F1 for *IV* relationships and function F3 for steady-state slow inactivation curves, *solid lines*) are described in the "Materials and methods"

Europe PMC Funders Author Manuscripts

Europe PMC Funders Author Manuscripts

Table 1

Comparison of sodium current activation, fast inactivation kinetics, cell capacitance and current density between skeletal myocytes and cardiomyocytes derived from different mouse strains

Strain			Activation			Current decay	Cell capacitance (pF)	Current density (pA/pF)
			$V_{0.5}$, mV	*K*, mV	V_{rev}, mV	Half-time (ms)		
Skeletal muscle	*BL6*	Neonatal early	*−32±2 (18)*	*9.5±0.4 (18)*	26±1 (18)	**0.86±0.06 (18)**	*17±1 (17)*	−66±6 (17)
	129	Neonatal early	*−32±1 (25)*	*10.0±0.3 (25)*	28±1 (25)	**0.84±0.05 (25)**	*14±1 (24)*	−77±7 (24)
	FVB	Neonatal early	*−24±1 (29)* $^{++\ **}$	*11.4±0.3 (29)* $^{++\ **}$	28±1 (29)	**0.68±0.04 (29)** $^{++\ *}$	*12±1 (25)* $^{++\ **}$	−66±6 (25)
	BL6	Neonatal late	*−36±1 (21)*	*8.9±0.4 (21)*	*28±1 (21)*	*1.02±0.07 (21)*	15±1 (19)	**−130±25 (19)**
	129	Neonatal late	*−39±2 (18)*	*8.5±0.5 (18)*	*30±1 (18)*	*1.05±0.05 (18)*	17±2 (15)	**−72±11 (15)**
	FVB	Neonatal late	*−30±2 (23)* $^{++\ **}$	*10.5±0.3 (23)* $^{++\ **}$	*24±1 (23)* $^{++\ *}$	*0.76±0.04 (23)* $^{++\ **}$	14± 1 (19)	**−69±4 (19)** *
	BL6	Adult	−42±1 (22)	8.7±0.3 (22)	27±1 (22)	1.17±0.07 (22)	15±1 (20)	−70±7 (20)
	129	Adult	−38±2 (13)	8.4±0.4 (13)	30±1 (13)	1.29±0.11 (13)	19±4 (12)	−59±6 (12)
	FVB	Adult	−38±2 (23)	9.0±0.4 (23)	29±1 (23)	1.11 ±0.09 (23)	18±1 (17)	−72±8 (17)
Cardiac	*BL6*	Neonatal	−36±2 (14)	*7.4±0.2 (14)*	18±2 (14)	1.08±0.06 (14)	**20±1 (9)** ^{oo}	−100±9 (9)
	129	Neonatal	−35±1 (14)	*7.0±0.3 (14)*	20±1 (14)	1.13±0.06 (14)	**16±1 (14)**	−95 ±7 (14)
	FVB	Neonatal	−37±2 (17)	*6.3±0.2 (17)* **	21 ±1 (17)	1.24±0.06 (17)	**18±1 (17)**	−88±7 (17)

The parameters were obtained by using the analyzing procedures and fitting functions (F1) described in “Materials and methods”. Current decay (at I_{max}) half-time is the time period between the current peak and the time point at which the current had decayed to 50%. Line “neonatal early” represents skeletal myocytes derived from neonatal mice, which were differentiated for 3–6 days (4±0.3, BL6; 5±0.1, 129; 4±0.1, FVB). Line “neonatal late” represents neonatal animal-derived skeletal myocytes, which were differentiated for 10–14 days (11±0.3, BL6; 11 ±0.3, 129; 11± 0.2, FVB). Line “adult” represents adult animal-derived skeletal myocytes differentiated for 10–14 days (10±0.1, BL6; 10±0.2, 129; 10±0.2, FVB). Line “neonatal” represents cardiomyocytes derived from neonatal animals, which were grown in GM for 1–4 days (2±0.2, BL6; 1 ±0.3, 129; 1 ±0.1, FVB). Values represent means±SE; *n* in parentheses indicate the number of experiments. Data in bold indicate that an ANOVA significance test revealed a significant difference ($p<0.05$) between the respective parameters of the three different mouse strains. Data in italics indicate that ANOVA revealed a highly significant difference ($p<0.01$) between the strains. Statistical comparisons between two groups were made using two-tailed Student's unpaired *t* tests.

$^{++}$Here, $p<0.01$ indicates a significant difference between FVB and 129.

*$p<0.05$

**$p<0.01$ indicate a significant difference between FVB and BL6.

^{oo}$p<0.01$ indicates a significant difference between BL6 and 129.

V0.5 The voltage at which half-maximum activation occurred, *K* the slope factor, V_{rev} the reversal potential

Europe PMC Funders Author Manuscripts

Table 2

Fast and slow inactivation parameters of skeletal myocytes and cardiomyocytes derived from different mouse strains

Strain			Fast inactivation		Slow inactivation		
			$V_{0.5}$, mV	*K*, mV	$V_{0.5}$, mV	*K*, mV	$Fract_{SI}$
Skeletal muscle	*BL6*	Neonatal early	−69±1 (24)	6.9±0.2 (24)	*−55±1 (7)* °°	12.3 ±1.3 (7)	0.70±0.06 (7)
	129	Neonatal early	−69±1 (23)	6.6±0.1 (23)	*−65±1 (8)*	11.3 ±1.0 (8)	0.69±0.04 (8)
	FVB	Neonatal early	−67±1 (21)	6.9±0.1 (21)	*−55±2 (10)* ++	9.7±0.4 (10)	0.71±0.02 (10)
	BL6	Neonatal late	**−71±1 (19)**	**6.7±0.3 (19)**	−57±2 (7)	13.4±1.6 (7)	*0.50±0.02 (7)* °
	129	Neonatal late	**−69±1 (30)**	**7.0±0.1 (30)**	−58±1 (20)	12.1 ±0.5 (20)	*0.60±0.02 (20)*
	FVB	Neonatal late	**−72±1 (26)** +	**7.3±0.1 (26)***	−52±2 (7) +	10.9±0.8 (7)	*0.67±0.03 (7)* **
	BL6	Adult	−75 ±1 (22)	7.1 ±0.2 (22)	−57±1 (13)	11.6±0.8 (13)	0.64±0.04 (13)
	129	Adult	−74±1 (17)	7.3±0.2 (17)	−57±2 (12)	12.6±0.8 (12)	0.61±0.03 (12)
	FVB	Adult	−71 ±1 (28)*	7.0±0.2 (28)	−53±1 (11)	12.1 ±0.6 (11)	0.62±0.02 (11)
Cardiac	*BL6*	Neonatal	−69±2 (16)	8.4±0.1 (16)	−59±3 (14)	**21.0±0.9 (14)** °	0.41±0.03 (14)
	129	Neonatal	−67±1 (21)	8.7±0.2 (21)	−58±2 (9)	**23.9±0.7 (9)**	0.41±0.04 (9)
	FVB	Neonatal	−68±1 (17)	8.0±0.2 (17)	−61 ±2 (11)	**20.6±0.7 (11)** ++	0.42±0.02 (11)

The parameters were obtained by using the analyzing procedures and fitting functions (F2 and F3) described in “Materials and methods”. Values represent means±SE; *n* in parentheses indicate the number of experiments. Data in bold indicate that ANOVA revealed a significant difference ($p<0.05$) between the respective parameters of the three different mouse strains. Data in italics indicate that ANOVA revealed a highly significant difference ($p<0.01$) between the strains. Statistical comparisons between two groups were made using two-tailed Student's unpaired *t* tests.

+ Here, $p<0.05$

++ $p<0.01$ indicate a significant difference between FVB and 129.

* $p<0.05$

** $p<0.01$ indicate a significant difference between FVB and BL6.

° $p<0.05$

°° p<0.01 indicate a significant difference between BL6 and 129.

V0.5 The voltage at which half-maximum inactivation occurred, *K* the slope factor, $Fract_{SI}$ the fraction of channels that can be slow inactivated

Europe PMC Funders Author Manuscripts

Table 3

TTX-resistant sodium current fractions in skeletal myocytes derived from different mouse strains

	Strain		TTX-resistant fraction
Skeletal muscle	*BL6*	Neonatal early	**0.30±0.04 (6)** $^{\circ}$
	129	Neonatal early	**0.40±0.03 (9)**
	FVB	Neonatal early	**0.31±0.02 (13)** $^{++}$
	BL6	Neonatal late	**0.29±0.04 (10)** $^{\circ}$
	129	Neonatal late	**0.40±0.03 (18)**
	FVB	Neonatal late	**0.28±0.06 (8)** $^{+}$
	BL6	Adult	0.40±0.03 (14)
	129	Adult	0.45±0.04 (10)
	FVB	Adult	0.43 ±0.04 (11)

The TTX-resistant current fraction represents the fraction of the total sodium current in 140 mM sodium bath solution, which remained during superfusion of the cells with a bath solution containing 1 μM TTX. Values represent means±SE; *n* in parentheses indicate the number of experiments. Data in bold indicate that ANOVA revealed a significant difference ($p<0.05$) between the respective parameters of the three different mouse strains. Statistical comparisons between two groups were made using two-tailed Student's unpaired *t* tests.

$^{+}$Here, $p<0.05$

$^{++}p<0.01$ indicate a significant difference between FVB and 129.

$^{\circ}p<0.05$ indicates a significant difference between BL6 and 129.